Data and Range-Bounded Polynomials in ENO Methods

Martin Berzins

SCI Institute, University of Utah, Salt lake City, Utah, USA

Abstract

Essentially Non-Oscillatory (ENO) methods and Weighted Essentially Non-Oscillatory (WENO) methods are of fundamental importance in the numerical solution of hyperbolic equations. A key property of such equations is that the solution must remain positive or lie between bounds. A modification of the polynomials used in ENO methods to ensure that the modified polynomials are either bounded by adjacent values (data-bounded) or lie within a specified range (range-bounded) is considered. It is shown that this approach helps both in the range boundedness in the preservation of extrema in the ENO polynomial solution.

Keywords: Data-Bounded Polynomials, Range-Bounded Polynomials, Essentially Non-Oscillatory Methods
2000 MSC: 35L03, 65M08, 65D05.

1. Introduction

An important class of methods for the numerical solution of hyperbolic equations are based upon Essentially Non-Oscillatory (ENO) methods and Weighted Essentially Non-Oscillatory (WENO) methods. There is an influential and substantial body of work on these methods see [7, 12]. The potential for high accuracy solutions makes the use of high order polynomials attractive, despite some challenges in the analysis of such methods. This is particularly true with regard to stability issues and the preservation of positivity in the solution.

The preservation of physical properties in the solution of hyperbolic equations such as positivity and consequently the avoidance of unphysical overshoots and undershoots in solution values is often seen as important when deriving algorithms for such equations. The standard definition used here for a positivity preserving scheme for the advection equation requires

(see [5]) that the numerical solution at time t_{n+1} be written in terms of the numerical solution at time t_n in the form

$$U_i(t_{n+1}) = \sum_j a_j U_j(t_n) \text{ where } \quad \sum_j a_j = C, \quad \text{and } a_j \geq 0 \ . \tag{1}$$

The constant C should ideally be one, [5]. With regard to ENO and WENO methods there have been a number of approaches proposed to address such issues. For example a modification to the ENO approach to enable the method to be Total Variation Diminishing (TVD) is provided in the preprint of Shu [11]. A slightly different approach so as to keep the ENO stencil closer to a linearly stable stencil is also described by Shu [13]. Balsara and Shu [1] construct specific high-order schemes. Shu points out in a recent survey of WENO methods it is difficult to generalize analysis of some of the methods beyond third order, [12]. Recently Zhang and Shu [15] have extended TVD WENO schemes to sixth order [15], by using a novel approach involving the exact integration of the solution in time. Perhaps most importantly a recent paper of Zhang and Shu [16] includes a novel limiter that when applied to the solution ensures that the solution lies between particular values:

$$m \leq U^I(x) \leq M. \tag{2}$$

We refer to this as a *Range-Bounded* approach.

One of the challenges in constructing methods that enforce such conditions is to be able to bound solutions consisting of high-order polynomials. In this paper the intention is to start from recent work on data-bounded polynomial interpolating functions s, [3, 4] and to consider if those approaches may be extended to bound the solution as in equation (2).

Sections 2,3 and 4 of this paper describe ENO methods and the data-bounded polynomial approach that will be used here. These results then make it possible to prove results about the range-bounded nature of higher order ENO type polynomials and to show numerical results on test problems that illustrate these results in Sections 5, 6 and 7. A summary of the results is provided in Section 8.

2. ENO Methods

Consider the advection equation with non-negative initial data:

$$\frac{\partial u}{\partial t} + a\frac{\partial u}{\partial x} = 0 \tag{3}$$

UU IR Author Manuscript

with appropriate boundary conditions on a spatial interval $[A, B]$. ENO schemes integrate this equation over the interval $[x_{i-1}, x_i]$ to get:

$$\frac{\partial \bar{u}_{i+1/2}}{\partial t} + a\frac{[u(x_i,t) - u(x_{i-1},t)]}{(x_i - x_{i-1})} = 0 \tag{4}$$

where the cell-averaged solution value $\bar{u}_{i+1/2}(t)$ is defined by

$$\bar{u}_{i+1/2}(t) = \frac{1}{(x_i - x_{i-1})}\int_{x_{i-1}}^{x_i} u(x,t)dx. \tag{5}$$

The ENO reconstruction function $w_i(x,t)$ is defined by:

$$w_i(x,t) = \int_{\bar{x}_{i-1}}^{x} u(x^*,t)dx^*, x \in [x_{i-1}, x_i], \tag{6}$$

where $\bar{x}_{i-1}$ is an arbitrary lower limit. This reconstruction function is related to the cell-averaged value by

$$w_i(x_i,t) - w_i(x_{i-1},t) = \bar{u}_{i+1/2}(t)(x_i - x_{i-1}). \tag{7}$$

From differentiating equation (6) it follows that

$$\frac{dw_i}{dx}(x_i,t) - \frac{dw_i}{dx}(x_{i-1},t) = u(x_i,t) - u(x_{i-1},t). \tag{8}$$

At the boundary $x = 0$ the appropriate solution value $U_0(t)$ is substituted for $u(x_{i-1}, t)$. Using this relation in equation (4) and integrating in time using the forward Euler method gives.

$$\bar{u}_{i+1/2}(t_{n+1}) = \bar{u}_{i+1/2}(t_n) - \frac{a\delta t}{(x_i - x_{i-1})}\left[\frac{dw_i}{dx}(x_i,t_n) - \frac{dw_i}{dx}(x_{i-1},t_n)\right]. \tag{9}$$

The derivatives of $\frac{dw_i}{dx}(x,t)$, are calculated by taking into account upwind directions, see [13]. For a more general p.d.e. we would have to evaluate flux function values using Riemann solvers etc. The ENO algorithm has the following steps:
(i) On each interval create initial values of $\bar{u}_{i+1/2}(t)$ by using exact or high-order quadrature based on the values $u(x,t)$.
(ii) Use equation (7) to create the first differences of the function $w_i(x,t)$.
(iii) Use these differences and subsequent differences to create a high order polynomial approximation on each interval to $w_i(x,t)$; we denote this polynomial by $w_i^*(x,t)$.
(iv) Calculate the derivatives of this polynomial $\frac{dw_i^*}{dx}(x_i,t)$ and $\frac{dw_i^*}{dx}(x_{i-1},t)$.
(v) Advance the solution in time using equation (9) with a sufficiently small timestep, δt, by using forward Euler or TVD Runge Kutta methods [7, 12].

3. ENO Divided difference polynomials

In calculating the required solution derivatives in equation (9) ENO methods [7, 12] use the divided difference form of polynomial interpolation, [9] in which $U[x_i] = U(x_i)$ and where subsequent divided differences are defined recursively by

$$U[x_i, x_{i+1}, ..., x_{i+k}] = \frac{U[x_{i+1}, x_{i+2}..., x_{i+k}] - U[x_i, x_{i+1}, ..., x_{i+k-1}]}{(x_{i+k} - x_i)}. \quad (10)$$

It will also be helpful later to define undivided differences by $U\{x_i\} = U(x_i)$ and where subsequent differences are defined recursively by

$$U\{x_i, x_{i+1}, ..., x_{i+k}\} = U\{x_{i+1}, x_{i+2}..., x_{i+k}\} - U\{x_i, x_{i+1}, ..., x_{i+k-1}\}. \quad (11)$$

ENO methods adaptively pick a stencil with the smallest divided differences. Consider the standard linear polynomial

$$U(x) = U[x_i] + (x - x_i)\ U[x_i, x_{i+1}]. \quad (12)$$

In the case that

$$|U[x_{i-1}, x_i, x_{i+1}]| > |U[x_i, x_{i+1}, x_{i+2}]|, \quad (13)$$

the quadratic ENO polynomial is then given by

$$U(x) = U[x_i] + (x - x_i)\ U[x_i, x_{i+1}] + (x - x_i)(x - x_{i+1})\ U[x_i, x_{i+1}, x_{i+2}]. \quad (14)$$

Otherwise the rightmost term is replaced by $(x - x_i)(x - x_{i+1})\ U[x_{i-1}, x_i, x_{i+1}]$.

There are many results about the stability and accuracy properties of ENO methods. While Harten et al. [8] show that the ENO approach may not result in oscillations in certain situations such behavior is not guaranteed. For example, although the standard ENO method does not always generate unphysical values, it is straightforward to create simple examples in which overshoots occur. For example consider a quadratic polynomial passing through three points $(x_i, y_i), i = 0, 1, 2$ and suppose that $(x_0, y_0) = (0, 0)$. The quadratic polynomial expansion about this point is then given by

$$y(x) = y_1\ [s(1 + (s - 1)(M - 1))] \quad (15)$$

where $s = x/(x_1 - x_0)$ and the ratio $M = (y_2 - y_1)/)(y_1)$. It is straightforward to calculate that if $M < -1$ and $M > 2$ then there are values of $y(x)$ that lie outside the range $[0, y_1]$.

In using the ENO polynomial approach to represent a cell-averaged function it is important to note that if the solution to the p.d.e. is non-negative then the cell-averaged function $w_i(x,t)$ is non-decreasing. Hence on physical grounds it is appropriate to represent this function by a data-bounded polynomial for which:

$$w_i(x_{i-1},t) \leq w_i(x,t) \leq w_i(x_i,t) \ \forall \ x \in [x_{i-1},x_i]. \tag{16}$$

This is the approach advocated by [3]. However a combination of positive and negative solution values may result in extrema in the cell-averaged function $w_i(x,t)$. Hence there is a need to construct a polynomial representation for this function that allows for extrema in the reconstruction function.

4. A Data-Bounded Polynomial Approach

The data-bounded approach of Berzins [3, 4] uses the ENO divided difference interpolation scheme in recursive form by defining the ratios of divided differences, for example, by

$$r^{[i,i+1,i+k+1]}_{[i-1,...,i+k]} = \frac{U[x_i,...,x_{i+k+1}]}{U[x_{i-1},...,x_{i+k}]}. \tag{17}$$

Such ratios, often of first divided differences are used as part of many very widely used positivity methods for solving compressible flow problems, see [14]. The main idea here is to use ratios of divided differences in constructing polynomials that may form part of high-order discretization methods. For example, when the next divided difference approximation to be computed incorporates a new point from the left x_{i-1}, it may be written in the form

$$U[x_{i-1},x_i,...,x_{i+k},x_{i+k}] \ = \ \frac{\left(1 - r^{[x_{i-1},...,x_{i+k-1}]}_{[x_i,...,x_{i+k}]}\right)}{x_{i+k} - x_{i-1}} U[x_i,x_{i+1},...,x_{i+k}]. \tag{18}$$

An alternative divided difference computed from $U[x_i,x_{i+1},...,x_{i+k}]$ is

$$U[x_i,x_{i+1},x_{i+2},...,x_{i+k+1}] \ = \ \frac{\left(r^{[x_{i+1},...,x_{i+k+1}]}_{[x_i,...,x_{i+k}]} - 1\right)}{x_{i+k+1} - x_i} U[x_i,x_{i+1},...,x_{i+k}]. \tag{19}$$

In this case the ENO scheme picks the next difference to be that in (18) if

$$\frac{\left(|1 - r^{[x_{i-1},...,x_{i+k-1}]}_{[x_i,...,x_{i+k}]}|\right)}{|x_{i+k} - x_{i-1}|} < \frac{\left(|r^{[x_{i+1},...,x_{i+k+1}]}_{[x_i,...,x_{i+k}]} - 1|\right)}{|x_{i+k+1} - x_i|}, \tag{20}$$

UU IR Author Manuscript

or picks that in (19) otherwise. In the approach of [3], providing that the values of $r_{[...]}^{[...]}$ satisfy the restriction

$$0 \leq r_{[...]}^{[...]} \leq 1, \tag{21}$$

then, if equation (21) holds we pick the next stencil point to be to the "left" i.e. x_{i-1} as in equation (10) and define λ_{k+1} by

$$1 \geq \lambda_{k+1} \;=\; \left(1 - r_{[x_i,\ldots,x_{i+k}]}^{[x_{i-1},\ldots,x_{i+k-1}]}\right) \geq 0. \tag{22}$$

Alternatively if equation (19) does not hold, then the next stencil point is picked to the "right", as in equation (20), x_{i+1} and define λ_{k+1} by

$$-1 \leq \lambda_{k+1} \;=\; \left(r_{[x_i,\ldots,x_{i+k}]}^{[x_{i+1},\ldots,x_{i+k+1}]} - 1\right) \leq 0. \tag{23}$$

For non-uniform meshes the values x_i, are defined in terms of a starting point x_0 by adding or subtracting multiples of the mesh spacing h so that the mesh points chosen by the ENO approach at each stage are denoted by x_i^e as defined by

$$x_i^e = x_0 + e_i h,\ i \geq 1, where\ h = (x_1 - x_0), \tag{24}$$

for some value e_i and where $e_1 = 1$ and if $e_i > 0$ then $e_i > 1$. At the ith stage of the ENO process let the leftmost and right most parts of the stencil in use may be defined as x_i^l and x_i^l, where

$$x_i^l = min(x_i^e, x_{i-1}^l), \quad x_0^l = x_0, \tag{25}$$

$$x_i^r = max(x_i^e, x_{i-1}^r), \quad x_0^r = x_0. \tag{26}$$

Defining a local co-ordinate, s, in the interval $[x_0, x_1]$ by:

$$s = \frac{x - x_0}{x_1 - x_0}, \tag{27}$$

allows the limited ENO polynomial, [3], to be written as:

$$U^l(x) = U[x_0] + [U(x_1) - U(x_0)]P_N(s). \tag{28}$$

$P_N(s)$ is the polynomial defined by:

$$P_N(s) = s + s(s-1)P_N^*(s) \tag{29}$$

where

$$P_N^*(s) = \frac{\bar{\lambda}_2}{D_2^*} + (s-e_2)\frac{\bar{\lambda}_3}{D_3^*} + (s-e_2)(s-e_3)\frac{\bar{\lambda}_4}{D_4^*} + ... \\ ... + (s-e_2)...(s-e_{N-1})\frac{\bar{\lambda}_N}{D_N^*}, \tag{30}$$

$$D_i^* = \prod_{j=2}^{i} D_j,\ D_i = (x_i^r - x_i^l)/(x_1 - x_0), \tag{31}$$

where $\bar{\lambda}_j = \prod_{k=2}^{j} \lambda_k$ and

$$-1 \le \bar{\lambda}_j \le 1. \tag{32}$$

It may be shown that (32) is equivalent to a restriction on undivided differences

$$-1 \le \frac{u\{x_j^l, ..., x_j^r\}}{u\{x_0, x_1\}} \le 1. \tag{33}$$

The original ENO polynomial has the same form as that in equation (30), but without any restriction on the values of $\bar{\lambda}_j$. in this case we denote the value of this polynomial equivalent to $P_N^*(s)$ by

$$\hat{P}_N^*(s) = \frac{\bar{\lambda}_2}{D_2^*} + (s-e_2)\frac{\bar{\lambda}_3}{D_3^*} + (s-e_2)(s-e_3)\frac{\bar{\lambda}_4}{D_4^*} + ... \\ ... + (s-e_2)...(s-e_{N-1})\frac{\bar{\lambda}_N}{D_N^*}, \tag{34}$$

where the values of $\bar{\lambda}_j$ are not assumed to be bounded. The following two theorems [3, 4] provide the boundedness results needed here.

Theorem 1 The interpolating function $U^I(x$ constructed using the ENO approach with limited ratios of divided differences as in equation (32) is data-bounded on a nonuniform mesh in that

$$Min(U(x_i), U(x_{i+1})) \le U^I(x) \le Max(U(x_i), U(x_{i+1})).$$

Theorem 2: The derivative of the interpolating function, $U^I(x)$, constructed using the modified ENO algorithm satisfies the equation:

$$\frac{dU^I(x)}{dx} = U[x_0, x_1]\ \left[1 + s(s-1)\frac{dP_N^*(s)}{dx} + (2s-1)P_N^*(s))\right]. \tag{35}$$

At the grid point $x = x_1$ this gives

$$\frac{dU^I(x_1)}{dx} = U[x_0, x_1]\,[1 + P_N^*(1)] \tag{36}$$

and again at the grid point $x = x_0$ gives

$$\frac{dU^I(x_0)}{dx} = U[x_0, x_1)] \left[1 - P_N^*(0)\right]. \tag{37}$$

5. Investigating Solution Behavior in ENO methods

While equations (36, 37) bound the ENO p.d.e. solution behavior at the edges of each interval they do not describe solution behavior in the interior of each element. In order to do this rewrite equation (30) as

$$P_N^*(s) = \frac{\bar{\lambda}_2}{D_2^*} + \sum_{j=2}^{N} \frac{\bar{\lambda}_{j+1}}{D_{j+1}^*} \prod_{i=2}^{j} (s - e_i) \tag{38}$$

and note that its derivative is

$$\frac{dP_N^*(s)}{ds} = \sum_{j=2}^{N} \frac{\bar{\lambda}_{j+1}}{D_{j+1}^*} \prod_{i=2}^{j} (s - e_i) \left[\sum_{i=2}^{j} \frac{1}{(s - e_i)}\right]. \tag{39}$$

The right side of equation (35) may then be written as

$$\begin{aligned}\left[1 + s(s-1)\frac{dP_N^*(s)}{dx} + (2s-1)P_N^*(s))\right] &= 1 + (2s-1)\frac{\bar{\lambda}_2}{D_2^*} \\ + \sum_{j=2}^{N} \frac{\bar{\lambda}_{j+1}}{D_{j+1}^*} \prod_{i=2}^{j} (s - e_i) &\left[s(s-1)\sum_{i=2}^{j} \frac{1}{(s - e_i)} + (2s-1)\right].\end{aligned} \tag{40}$$

In order to find values for $\bar{\lambda}_{j+1}$ that limit the derivative we use the following approach. In investigating the boundedness of the derivative defined by equation (35)we assume that the derivative is smaller at $s = 0$ than at $s = 1$. The alternative case may be dealt with similarly. Subtracting 1 from the right side of (40) gives the following equation that must be satisfied for boundedness of the derivative of the data bounded polynomial.

$$\begin{aligned}-\frac{\bar{\lambda}_2}{D_2} - \sum_{j=2}^{N} \frac{\bar{\lambda}_{j+1}}{D_2} \prod_{i=2}^{j} \frac{(-e_i)}{D_{i+1}} \leq \\ (2s-1)\frac{\bar{\lambda}_2}{D_2} + \sum_{j=2}^{N} \frac{\bar{\lambda}_{j+1}}{D_2} \prod_{i=2}^{j} \frac{(s - e_i}{D_{i+1}}) \left[s(s-1)\sum_{i=2}^{j} \frac{1}{(s - e_i)} + (2s-1)\right] \\ \leq \frac{\bar{\lambda}_2}{D_2} + \sum_{j=2}^{N} \frac{\bar{\lambda}_{j+1}}{D_2} \prod_{i=2}^{j} \frac{(1 - e_i)}{D_{i+1}}.\end{aligned} \tag{41}$$

While it is not straightforward to show that this is true numerical experiments show that many standard cases do yield bounded derivatives. For example, let Case 1 consist of a stencil successively adding points to the right. In this case for an even mesh it follows that

$$e_i = i, D_i = i + 1. \tag{42}$$

Case 2 The second case consists of a stencil successively adding points to the right. In this case for an even mesh it follows that

$$e_i = -i + 1, D_i = i + 1. \tag{43}$$

Figure 1 illustrates the behaviors of the polynomials for Cases 1 and 2 in which the values of λ_j were chosen so as to give the largest possible values positive values close to $s = 0$. In these cases and many others the polynomial derivatives often do not seem to have extrema in the interval. In order to show situations in which the solution is data-bounded but the derivatives are not we consider the following two cases. In each case the derivative has the form

$$\frac{dU^I(x)}{dx} = U[x_0, x_1]\frac{dP_N}{ds}. \tag{44}$$

The two cases to consider based on [4] namely those when $e_i = 0$ and $e_i = 1$, correspond to the bounding polynomials for $P_N(s)$. In both cases $D_i = 1 \forall i$. These are the limiting cases representing the limit of $e_i = 1 + \delta_i$ or $e_i = -\delta_i$ for δ_i small. In these two cases have the following derivatives when we take $\delta_i = 0$.

$$\frac{dP^N(x)}{ds} = \left[1 + (2s-1)\bar{\lambda}_2 + \sum_{j=2}^{N} \bar{\lambda}_{j+1} s^{j-1}(sj + s - j)\right] \tag{45}$$

and

$$\frac{dP^N(x)}{ds} = \left[1 + (2s-1)\bar{\lambda}_2 + \sum_{j=2}^{N} \bar{\lambda}_{j+1} (s-1)^{j-1}(sj + s - 1)\right]. \tag{46}$$

For the above two polynomials, with values of $\bar{\lambda}_i = \pm 1$ the curves are copies of a single curve reflected about $y = 0$ or $x = 0.5$. The single curve itself is given by the bracketed term [...] in equation (45) and is shown in Figure 2. In the left case when $\lambda_i = 1 \forall i$ the derivatives are bounded but in the right case when a change is made so that $\lambda_2 = -1$ the derivatives are not bounded

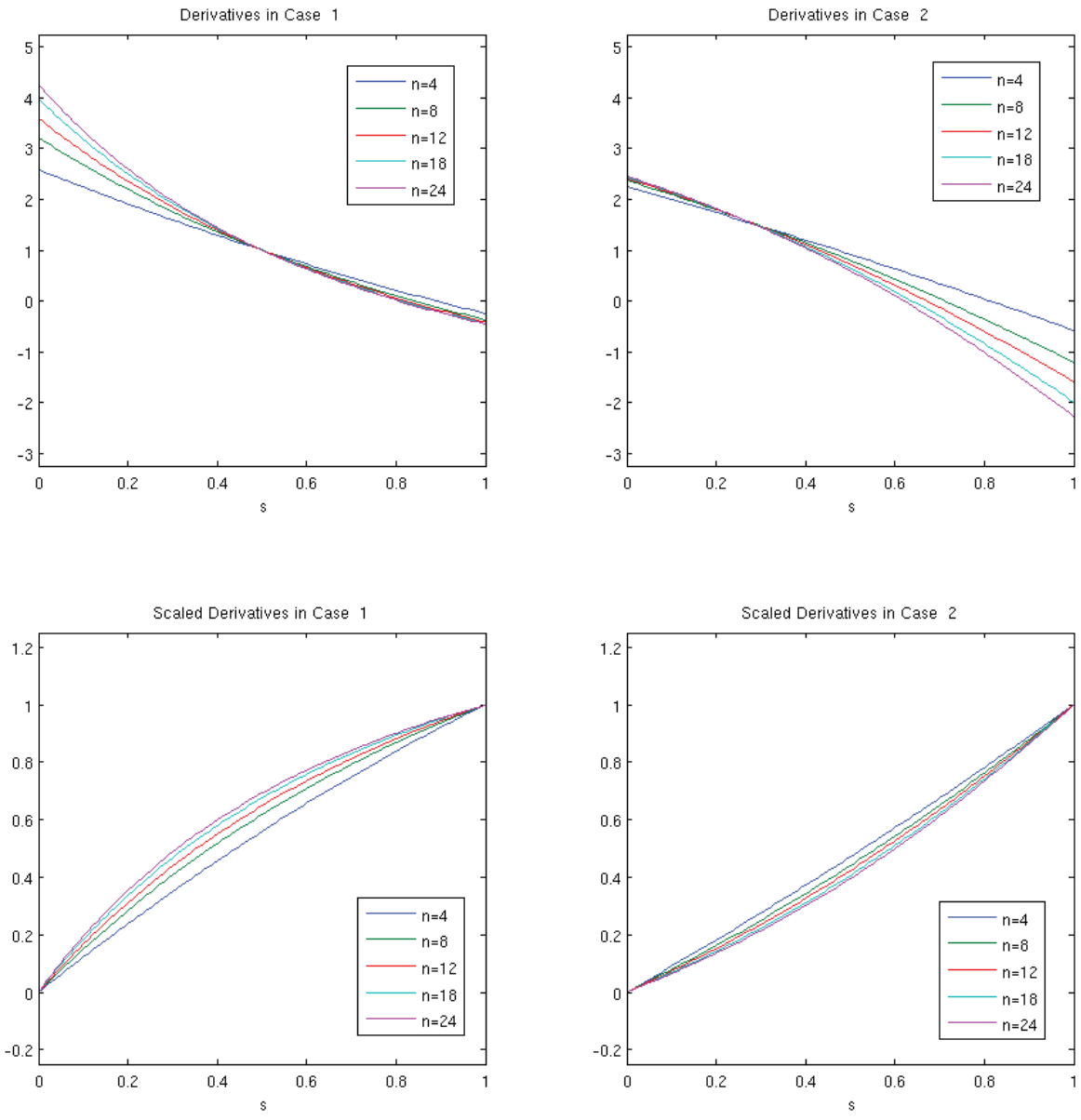

Figure 1: Graphs of Derivatives and Scaled Derivatives

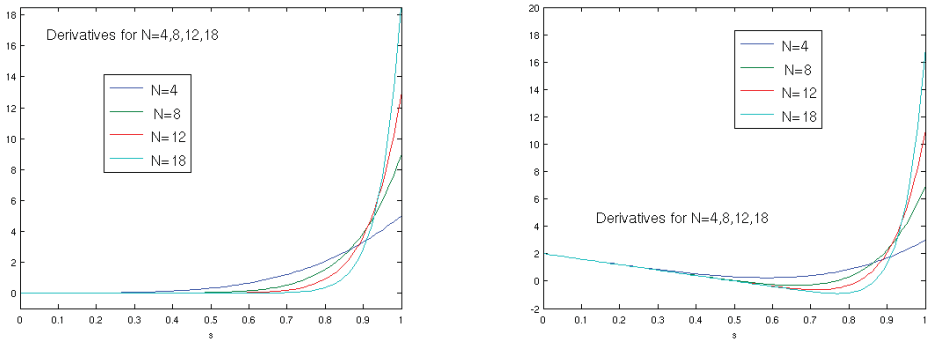

Figure 2: Derivatives for N=4,8,12,18 with $\lambda_i = 1$ and then with the change $\lambda_2 = -1$

by the values at the edge of the interval. This behavior is not surprising as in this case

$$P^N(s) = \left[s - (s^2 - s) + (s^2 - s) \sum_{j=2}^{N} s^{j-1} \right]. \tag{47}$$

The polynomial $P^N(s)$ in this case is monotone on $[0, 1]$ as it may be written as:

$$P^N(s) = s - 2(s^2 - s) - s(1 - s^N). \tag{48}$$

The differential of this polynomial is

$$\frac{dP^N(x)}{ds} = -4s + 2 + (N + 1)s^N \tag{49}$$

which has a minimum at $s = (4/(N(N+1)))^{\frac{1}{N-1}}$. In this case it would seem that further restrictions are needed on λ_i to ensure that this polynomial is monotone on $[0, 1]$. This issue is explored in Section 8. The conclusion to be drawn from these experiments is that while it perhaps appears relatively unlikely for extrema to be created in the derivatives of the type of data-bounded polynomials considered here, it is not impossible.

6. Range-Bounded Polynomial Approximations.

The next step is to allow for extrema by considering range-bounded polynomial approximations for the reconstruction function. This is done by modifying the bounded polynomial approach [4] in a way that allows a

bounded extremal value to be created in the same way [16] as in equation (2). The first issue is that it is necessary to determine whether the polynomial is close to the upper bound or lower bound. In doing so we use the result from Berzins [4] that

$$s^N \leq s + s(s-1)P_N^*(s) \leq 1 - (1-s)^N \tag{50}$$

which after some straightforward manipulation may be written as

$$-\frac{1-(1-s)^{N-1}}{s} \leq P_N^*(s) \leq \frac{1-s^{N-1}}{1-s}. \tag{51}$$

From the bounds in equation (51 we get a general bound on $P_N^*(s)$ and in the case of $s = 0$ and $s = 1$ L'Hopital's rule is used to calculate the bounds, [4].

$$-(N-1) \leq P_N^*(0)) \leq 1 \tag{52}$$

and

$$-1 \leq P_N^*(1)) \leq N-1. \tag{53}$$

Thus also showing that the derivatives of that data bounded reconstruction function as defined by equations (36) and (37) are both positive, if the cell average is positive, and hence so are the ENO solution values as defined by equations (8). In order to bound a polynomial between some pre-defined range values we start from the approach given by equations (67),(68) and (69) of [4] but with the inclusion of the small linear term $u[x_0, x_1]$. With this in mind, consider modifying the bounds for $\bar{\lambda}_i$ to get a parameter $\bar{\lambda}_i^*$ such that

$$-b \leq \bar{\lambda}_i^* \leq b \tag{54}$$

and then assuming that

$$\bar{\lambda}_i^* = b\bar{\lambda}_i \tag{55}$$

it is possible to define a polynomial by

$$U_m^M(x) = U_0 + [U_1 - U_0]s + bs(s-1)P_N^*(s) \tag{56}$$

where the parameter b is yet to be specified, but when known is introduced by using the bounds (54) for $\bar{\lambda}_i^*$ and using this in place of $\bar{\lambda}_i$ in $P_N^*(s)$. From equation (50) above it now follows that

$$U_0 + [U_1 - U_0]s - Q_N^-(s) \leq U_m^M(x) \leq U_0 + [U_1 - U_0]s + Q_N^+(s) \tag{57}$$

where

$$Q_N^-(s) = b(s - s^N) \tag{58}$$

and

$$Q_N^+(s) = b((1-s) - (1-s)^N). \tag{59}$$

Figure 3 shows how the function $Q_N^+(s)$ can achieve a maximum by varying

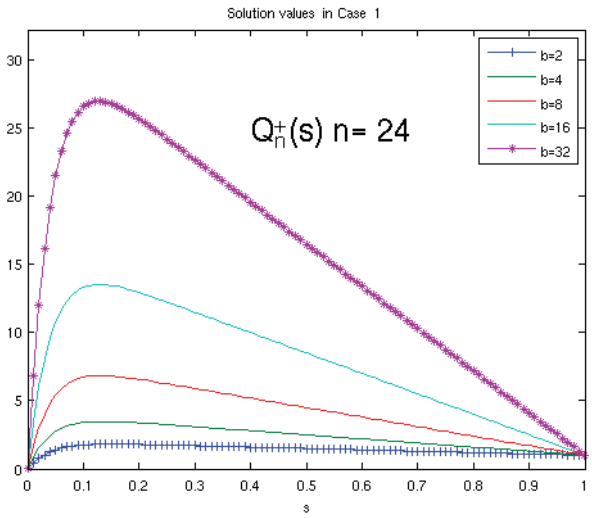

Figure 3: Values of Q_N^+ for varying b

the value b from $b = 2$ to $b = 32$ for a value of $N = 24$. The figure shows that the bound is asymptotic and for example when $b = 32$, the actual bound reached by $Q_N^+(s)$ is about 27. Similar results hold for minima with $Q_N^-(s)$.

6.1. Approximating Extremal Values

In order to enforce condition on boundedness it is important to look at the properties of the bounding functions. The extrema of the left bounding function in equation (57) are defined as the solutions to the equations:

$$U_0 + [U_1 - U_0]s - b(s - s^N) = m, \tag{60}$$

$$[U_1 - U_0] - b(1 - Ns^{N-1}) = 0. \tag{61}$$

Multiplying the second equation by s and subtracting it from the first gives

$$b = \frac{U_0 - m}{s^N(N-1)}. \tag{62}$$

Substituting this back in equation (61) for b gives

$$[U_1 - U_0] - \frac{U_0 - m}{s^N(N-1)}(1 - Ns^{N-1}) = 0, \tag{63}$$

which may also be written as

$$R - \frac{(1 - Ns^{N-1})}{s^N(N-1)} = 0, \tag{64}$$

where $R = [U_1 - U_0]/(U_0 - m)$ represents the reciprocal of the relative distance to the minimum value m from U_0 as compared to the distance between U_0 and U_1. With an appropriate sign change equation (62) may be written as

$$b = \beta(U_0 - m) \tag{65}$$

where $\beta = \frac{1}{\bar{s} - \bar{s}^N}$ and $\bar{s}$ is the value of s that satisfies equation (63) the values of β are tabulated below from a numerical calculation. Table 1 shows how

N/R	0	1/2	1/4	1/8	1/16	1/32
4	2.1	2.7	2.4	2.3	2.2	2.2
6	1.7	2.3	2.0	1.8	1.8	1.7
8	1.5	2.1	1.8	1.7	1.6	1.6
10	1.4	2.0	1.7	1.6	1.5	1.5
14	1.3	1.8	1.6	1.4	1.4	1.3
18	1.2	1.8	1.5	1.4	1.3	1.3

Table 1: Values of β for different values of N and R

the value of b should be set in relation to U_0 and m in the case of a minimum. A similar analysis yields similar results for a maximum.

6.2. Numerical Examples

In this numerical example we consider four approaches to polynomial approximation:

- Original: in which a data bounded approach is used as in [4] based on equation (21).
- Improved: in which zero values of differences are allowed, (32).
- Bounded Extrema: in which extrema are detected and the approach of equation (56), with $b = 1.2$
- New Extrema Allowed: in which we simply use the original ENO polynomial with no limiting when extrema are detected.

UU IR Author Manuscript

The test problem is Runge's function $1/(1+25x^2)$, with NPTS evenly data points spaced so as to exclude the extremal value at $x = 0$. In Table 2, NP is the number of points used to define the polynomial, or the order plus one. Table 2 shows that allowing extrema within bounds gives much greater

Method	NPTS	L2 Error	L∞ Error	Max NP	Min NP	Avg NP
Original	6	3.4e-3	5.0e-1	4	2	3
No New	14	5.7e-4	1.3e-1	8	3	7
Extrema	30	8.6e-5	2.9e-2	17	3	15
Allowed	60	1.5e-5	7.1e-3	34	3	32
	120	2.6e-6	1.3e-4	57	3	53
Improved	6	3.1e-3	4.5e-1	3	2	3
No New	14	3.2e-4	7.4e-2	7	2	6
Extrema	30	1.8e-5	6.1e-2	16	2	14
Allowed	60	9.4e-7	4.3e-3	33	2	31
	120	4.2e-8	2.8e-5	57	3	53
	6	3.0e-3	4.7e-1	4	2	3
Bounded	14	2.5e-4	5.8e-2	7	4	6
Extrema	30	3.1e-6	1.1e-3	16	8	14
Allowed	60	3.0e-7	1.2e-4	33	17	31
	120	1.1e-8	6.4e-6	120	38	53
	6	3.0e-3	4.3e-1	6	2	3
New	14	1.8e-4	4.3e-2	14	4	7
Extrema	30	2.6e-6	5.2e-4	30	10	15
Allowed	60	3.0e-7	1.2e-4	60	17	32
	120	1.1e-8	6.4e-6	120	38	53

Table 2: Approximation of Runge's Function With and Without Extrema Creation

accuracy than truncating extrema. The table also shows the difference between ways of treating λ. The original approach stopped the series when there was a zero value of a divided difference or that difference was too large, while the new method requires only that $\bar{\lambda}$ be bounded as in equation (32).

Another comparison that is particularly relevant to hyperbolic equations is to use the solution from Burgers equation with the initial condition

$$u(x,0) = sin(\pi x), x \in [0,1]. \tag{66}$$

This is solution 5.2 in the solutions provided by Benton and Platzman [2]. In this case the solution is evaluated by freely available matlab code of

UU IR Author Manuscript

Burkhardt [6], with the viscosity parameter set to 0.005. The solution at different time levels is shown on Figure 4. The results of applying the ENO

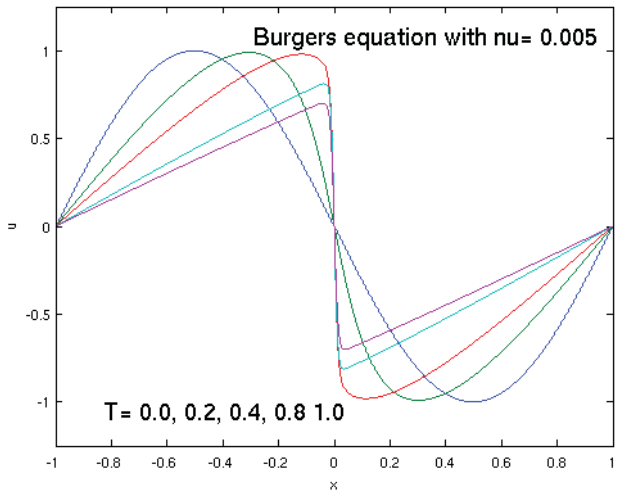

Figure 4: Burgers Equation Exact Solution

approach to the solution values at $T = 0.8$ are shown in Figure 5. For clarity only the section around the steep front is shown. The numerical results in Table 3 show that with the new approach it is possible to use a polynomial degrees of six to twelve instead of just two at extrema. As this is only at two extremal points the difference to the error norm is slight. Nevertheless this shows that it is possible to approximate smooth extrema without order reduction down two. It is also worth remarking that Even where both methods use a polynomial of degree 2 (NPTS = 30) the new approach uses this polynomial in fewer intervals.

7. Comparison With Zhang-Shu Approach.

With obvious changes of notation the method of [16] defines a limited polynomial for the derivative of the reconstruction function by

$$\frac{dU^Z(x)}{dx}(s) = U[x_0, x_1] \; + \theta \; U[x_0, x_1] \left[s(s-1)\frac{d\hat{P}_N^*(s)}{dx} + (2s-1)\hat{P}_N^*(s)) \right], \tag{67}$$

where the value of θ is defined by the limiter of [10] as

$$\theta = min \left\{ \left| \frac{M - U[x_0, x_1]}{M_j - U[x_0, x_1]} \right|, \left| \frac{m - U[x_0, x_1]}{m_j - U[x_0, x_1]} \right|, 1 \right\} \tag{68}$$

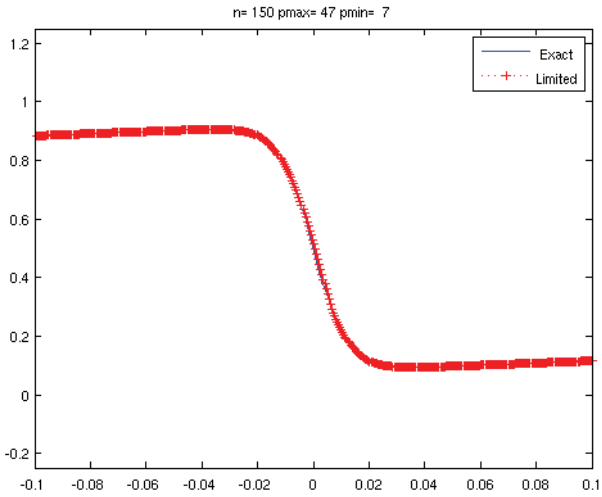

Figure 5: Burgers Equation ENO Polynomial Solution N = 150

with

$$M_j = \underset{x\in[x_0,x_1]}{\text{Max}} \frac{dU^I(x)}{dx}, m_j = \underset{x\in[x_0,x_1]}{\text{Min}} \frac{dU^I(x)}{dx}, \tag{69}$$

and the polynomial $\hat{P}^*_N(s)$ as defined in equation (34). has no restrictions on the values of $\bar{\lambda}_j$. In practice approximations to M_j and m_j are used as it is time consuming to compute these values otherwise. Even with these approximations it is still necessary to compute derivatives such as those in (67) at a significant number of quadrature points in the interval, [16].

From the linearity of the limiter of [16] it follows that this limiter applied to the derivative is identical to limiting the polynomial

$$U^M_m(x) = U_0 + [U_1 - U_0]s + b[U_1 - U_0]s(s-1)\hat{P}^*_N(s) \tag{70}$$

with $b = \theta$ and then differentiating, where again $\hat{P}^*_N$ has no restriction on the values of $\bar{\lambda}_j$. From this it follows that if:

$$\theta \leq 1/(\underset{j}{\text{Max}}\,|\bar{\lambda}_j|), \tag{71}$$

then this approach is similar to the data-bounded polynomial of [4], as this limiting approach is one way of ensuring that all the values of $\bar{\lambda}_j$ are less than one. The main difference between the approaches is that [4] truncates the polynomial after a value of $\bar{\lambda}_j$ is too large.

Method	NPTS	L1 Error	Max NP	Min NP	Avg NP
Original	30	8.6e-3	16	3	16
No New	60	2.9e-3	23	3	18
Extrema	90	9.8e-4	26	3	24
Allowed	120	3.6e-4	40	3	37
	150	1.8e-4	47	3	43
	30	8.5e-3	16	3	16
Bounded	60	2.7e-3	23	13	18
Extrema	90	8.3e-4	29	9	24
Allowed	120	3.4e-4	40	8	38
	150	1.5e-4	47	7	44

Table 3: Approximation of Runge's Function With and Without Extrema Creation

8. Bounded Derivative Values

The Zhang-Shu approach makes it possible to bound the derivatives of the ENO polynomial with respect to upper and lower solution bounds. As this is done by a sophisticated choice of $\bar{\lambda}_j$ it is natural to ask if it possible to choose values of $\bar{\lambda}_j$ so that the boundedness equation (41) holds. In order to ascertain whether or not such a condition might hold experiments were conducted by first modifying equation (41) by subtracting the left side from both the center and righthand terms and then dividing by the new right term to get, after some further simpifications, the inequality

$$0 \leq Z_n(s) \leq 1, \tag{72}$$

where

$$Z_n(s) = \frac{s + \sum_{j=2}^{N} \frac{\bar{\lambda}_{j+1} i}{2} \left(\prod_{i=2}^{j} \frac{(s-e_i)}{D_{i+1}} \right) \left[\sum_{i=2}^{j} \frac{(s^2-s)}{(s-e_i)} + 2s - 1 \right] + \prod_{i=2}^{j} \frac{(-e_i)}{D_{i+1}} \Big)}{1 + \sum_{j=2}^{N} \frac{\bar{\lambda}_{j+1}}{2} \left(\prod_{i=2}^{j} \frac{(1-e_i)}{D_{i+1}} + \prod_{i=2}^{j} \frac{(-e_i)}{D_{i+1}} \right)}$$

It is possible to derive a similar form when the derivative at $s = 0$ is larger than that at $s = 1$. Motivated by the examples of Berzins [4] in which the most problematical cases are those with points very close to $s = 0$ or $s = 1$ we investigated polynomials close to those in equations (45) and (46). In those cases even by placing severe restrictions on $\bar{\lambda}_j$ it was still not possible to get data bounded derivatives that satisfy equation (72). As such meshes are extreme and may not encountered in practical applications it is natural to

ask if it is possible to obtain monotone derivatives if a restriction is placed on $\bar{\lambda}_j$. A computational investigation of this was undertaken by random generation of the mesh points used by the ENO polynomial, the direction of the stencil and whether $\bar{\lambda}_j$ is positive or negative. The results for 400 randomly generated ENO polynomials with the restriction

$$|\bar{\lambda}_j| \leq Fac, \tag{73}$$

are shown in Figure 6 in which the left figure shows the values of $Z_n(s)$ for $Fac = 1.0$. The numerous data points outside the range $[0, 1]$ indicate that the derivatives are not bounded for those cases. Experiments using $Fac = 0.1$ generate seem bounded derivatives and provide insight on how to produce bounded derivatives if the mesh used by the ENO polynomial does not vary dramatically. From equation (40) and Theorem 1 a bounded

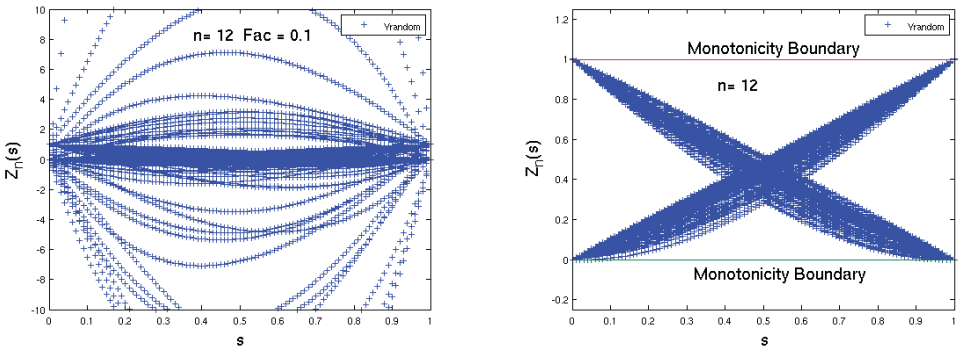

Figure 6: Random Polynomial Derivatives with $|\lambda_i| = \frac{1}{i}, \forall i > 2$

derivative polynomial may be found providing that

$$|\bar{\lambda}_{j+1}| \left| s(s-1) \sum_{i=2}^{j} \frac{1}{(s-e_i)} + (2s-1) \right| \leq 1. \tag{74}$$

Providing that the mesh varies sufficiently slowly that $|s - e_i| \geq 0.25$, say, then a sufficient condition for this is

$$|\bar{\lambda}_{j+1}| \left| \frac{(j-1)}{4} \underset{i}{max} \left\{ \frac{1}{|s-e_i|} \right\} + 2 \right| \leq 1, \tag{75}$$

or

$$|\bar{\lambda}_j| \leq \frac{1}{j}. \tag{76}$$

UU IR Author Manuscript

It is also necessary for the values of the points e_i to be distinct. Applying this approach to the random polynomials yields the results in the righthand figure of Figure 6. This figure shows that this limiting restriction on the values of $\bar{\lambda}_{j+1}$ yields bounded derivative values for the reconstruction function and hence data bounded solution values for the p.d.e. in the case of the random polynomials that satisfy the restriction $|s - e_i| \geq 0.25$. It is also necessary for the values of the points e_i to be distinct and so the restriction $|e_{i+1} - e_i| \leq 0.1$ was used in the experiments. These promising results show that this topic merits further study.

9. Summary

In this paper the data-bounded approach of [4] has been extended to the idea of range-bounded polynomials. This range-bounded approach has been shown to improve the accuracy of polynomial approximations to extrema in a controlled way. The relationship between this approach and the limiter of [16] has been established. A new boundedness limiter for derivatives of the ENO polynomial has been discovered. These results should help to make it possible to construct new limiters in the future.

Acknowledgement

The author would like to thank Allen Tesdall for his help and encouragement with this paper.

References

[1] Balsara D.S. and Shu C.W. Monotonicity preserving weighted essentially non-oscillatory schemes with increasingly high order of accuracy. *Journal of Computatational Physics* **160**:405-452 (2000).

[2] Benton E.R and Platzman G.W. A Table of Solutions of the On eDimensional Burgers Equation. *Quartely of Applied Mathematics.* **July**:195-212, 1972.

[3] M. Berzins, *Adaptive polynomial interpolation on evenly spaced meshes*, SIAM Review **1** (2007), no. 4, 624–627.

[4] Berzins M. Data-Bounded Polynomials and Preserving Positivity in High Order ENO and WENO Methods *Numerical Algorithms*, Vol. 55, No. 2, pp. 171. 2010.

UU IR Author Manuscript

[5] Borisov V.S. and Sorek S. On monotonicity of difference schemes for computational physics. *SIAM Journal of Scientific Computing* **25**:1557-1584, 2004.

[6] `http://people.sc.fsu.edu/~jburkardt/m_src/burgers_solution/burgers_solution.html`

[7] Cockburn B, Karniadakis GE, Shu C-W. (eds). *Advanced Numerical Approximation of Nonlinear Hyperbolic Equations. Lecture Notes in Mathematics 1697* Springer Berlin Heidelberg, 2000; pp 325–418.

[8] Harten,A. and Osher,S. and Engquist,B. and Chakravarthy,S. R., Some results on uniformly high-order accurate essentially nonoscillatory schemes, Applied Numerical Mathematics, 2, 3-5, pp.347-377. 1986,

[9] Hildebrand F.B. *Introduction to Numerical Analysis.* McGraw-Hill Book Company Inc 1956;

[10] X.-D. Liu and S. Osher, Non-oscillatory high order accurate self similar maxi- mum principle satisfying shock capturing schemes, SIAM Journal on Numerical Analysis, 33, (1996), pp.760-779.

[11] C.-W. Shu, TVD properties of a class of modified ENO schemes for scalar conservation laws, IMA Preprint Series 308 (1987), University of Minnesota.

[12] Shu C-W . High order WENO schemes. *SIAM Review* March 2009; 51, 82-126.

[13] C.-W. Shu, Numerical experiments on the accuracy of ENO and modied ENO schemes, *Journal of Scientific Computing*, 5, (1990), pp.127-149.

[14] Waterson N.P. and Deconinck H. Design Principles for bounded higher-order convection schemes - a unified approach. *Journal of Computational Physics* 2007; 224: 182-207.

[15] X. Zhang and C.-W. Shu, A genuinely high order total variation diminishing scheme for one-dimensional scalar conservation laws, SIAM Journal on Numerical Analysis, 48, (2010), pp.772-795. ‘

[16] X. Zhang and C.-W. Shu, On maximum-principle-satisfying high order schemes for scalar conservation laws, Journal of Computational Physics, 229, (2010), pp.3091-3120.